INSTITUTE OF THEORETICAL AND EXPERIMENTAL PHYSICS.
THE STATE COMMITTEE OF THE USSR FOR THE UTILIZATION OF ATOMIC ENERGY

Report 859

A STUDY OF THE REACTION $\pi^- + p \to n + \pi^+ + \pi^-$ AT AN INITIAL π^--MESON MOMENTUM OF 40 GeV

(proposed experiment)

B.P. Barkov, V.V. Vladimirskij,
Yu.V. Katinov and A.I. Sutormin

Moscow 1971

Translated at CERN by R. Luther
(Original: Russian)
Not revised by the Translation Service

(CERN Trans. 71-43)

Geneva
October 1971

INTRODUCTION

It is proposed to measure and determine the dependence of the differential cross-section $\frac{d\sigma}{dt}$ on the four-momentum t in the reaction

$$\pi^- + p \rightarrow n + \pi^+ + \pi^-$$

at an initial π^--meson momentum of 40 GeV/c; the t range is (0,04-0,40) $(GeV/c)^2$; the value of the invariant mass M_0 in the $\pi^+\pi^-$ system is

$$0{,}28 \leq M_0 \leq 3{,}0 \ GeV/c^2$$

The neutrons are recorded by a hodoscope system consisting of 8 scintillation counters, situated at (60-80)° to the direction of the incident π^--meson in the laboratory system. The neutron's time of flight is measured over L=3 m and the number of the counter triggered is fixed, i.e. θ of the lab. neutron. A momentum analysis of the $\pi^\pm$-mesons is performed in a MAGIK-6 spectrometer.

A diagram of the apparatus and the trigger's electronic logic are shown in Fig. 1.

We should point out that the device can be used to study not only the reaction

$$\pi^- + p \rightarrow n + \pi^+ + \pi^-$$

but also the processes

$$\begin{aligned} \pi^- + p &\rightarrow n + m(\pi^+\pi^-) + k\pi^0 \\ &\rightarrow n + m(K^+K^-) + k\pi^0 \\ &\rightarrow n + m(p\bar{p}) + k\pi^0 \\ &\qquad m \geq 0,\ k > 0 \\ &\qquad m > 0;\ k \geq 0 \end{aligned}$$

and $\pi^- + p \longrightarrow n + M_0$

where M_0 is the neutron's missing mass.

1. Existing data on the dynamics of the reaction $\pi^- + p \to n + \pi^+ + \pi^-$

A study of σ_{tot}, $\frac{d\sigma}{dt}$ in the reaction

(1.1) $$\pi^- + p \longrightarrow n + \pi^+ + \pi^-$$

and also of the partial cross-sections σ^i_{tot} , $\frac{d\sigma^i}{dt}$ in the reaction

(1.1') $$\pi^- + p \longrightarrow n + \mathcal{X}_i$$ where

$\mathcal{X}_i$ is the neutral component of the meson resonance, is interesting from the point of view of the theory of complex momenta.

If the reaction π^- + p follows the diagram

(1.2)

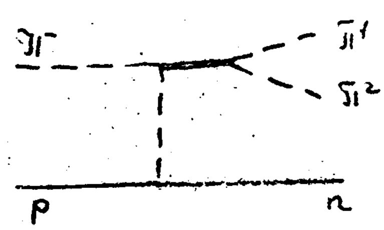

then the energy dependence of the cross-section may be described by the formula (.1/)

(1.3) $$\sigma \simeq P_i^{(2\alpha(0)-2)}$$, where

P_1 is the primary momentum of the π^--meson in the laboratory system, and

(1.4) $$\alpha(0) \simeq 0 \text{ for a } \pi \text{ pole exchange}$$
$$\alpha(0) \simeq 0{,}5 \text{ for a } \rho \text{ , } A_2 \text{ pole exchange}$$

Clearly, for (1.1) reactions the (1.2) diagram is only possible for π and A_2 charged poles and for (1.1), moreover, a ρ-pole exchange is possible if the resonance's g parity is negative.

In paper /2/, reaction (1.1) was studied at a primary momentum P_i = 11 GeV/c. The following cross-section was obtained

(1.5) $\sigma_{tot} = (0,7 \pm 0,1)$ mb.

(1.1) channels were also separated for ρ^0, f^0 and g^0 .

(1.6)
$$\sigma_{tot}(\rho^0 n) = (110 \pm 14) \text{ microbarn.}$$
$$\sigma_{tot}(f^0 n) = (75 \pm 14) \text{ microbarn.}$$
$$\sigma_{tot}(g^0 n) = (55 \pm 14) \text{ microbarn.}$$

Paper /2/ also presents a table of cross-sections for reaction (1.1) where P_i = (1,23 - 16,0) GeV/c. From this table, and using the data in paper /3/, at P_i = 16 GeV/c, it is possible to do the same as the authors of paper /3/ and deduce the energy dependence of $\sigma_{tot}(\pi^- p \rightarrow n \pi^+ \pi^-)$

(1.7)
$$\sigma_{tot} \sim p^{-1,3}$$

This dependence may be expected to continue into the higher energies, or the decay may slow down as the π pole dies out.

Paper /3/ gives the cross-sections

(1.8)
$$\sigma_{tot}(\pi^- p \rightarrow n \pi^+ \pi^-) = (0,40 \pm 0,08) \text{ mb.}$$

the partial cross-sections of reaction (1.1) with the production of a ρ^0-meson

(1.9)
$$\sigma(\pi^- p \rightarrow n \rho^0) = (52 \pm 13) \text{ microbarn.}$$

of a f^0 meson
$$\sigma(\pi^- p \rightarrow n f^0) = (38 \pm 9) \text{ microbarn.}$$

and the upper limit to the cross-section for the production of a g°-meson

(1.9) $$\sigma(\pi^- p \to n g^{\circ}) \leq (25 \pm 6) \text{ microbarn.}$$

The dependence on $|t|$ $\frac{d\sigma}{d\sigma}$ of reaction (1.1) and also of reaction (1.1') with the production of a ρ° and an f° is in good agreement with the predictions of the OPE and OPEA models.

We note that both in paper /2/ and in paper /3/ the dependence of $\frac{d\sigma}{dt}(\pi^- p \to n\pi^+\pi^-)$ on /t/ is satisfactorily described by the formula

(1.10) $$\frac{d\sigma}{dt} \sim e^{-\lambda|t|} \quad , \quad \lambda \simeq 10\,(GeV/c)^{-2}$$

and λ does not decrease as P_i increases. Drawing on previously published data, the authors of /3/ conclude that $\sigma(\pi^- p \to n\pi^+\pi^-)$, $\sigma(\pi^- p \to n\rho^{\circ})$ and $\sigma(\pi^- p \to n f^{\circ})$ depend on P_i

(1.11) $$\begin{cases} \sigma_{tot}(\pi^- p \to n\pi^+\pi^-) \sim p_i^{-1,3} \\ \sigma(\pi^- p \to n\rho^{\circ}) \sim p_i^{-2} \\ \sigma(\pi^- p \to n f^{\circ}) \sim p_i^{-2} \end{cases}$$

The statistics in paper /3/ are based on 573 reaction (1.1) events.

II. The kinematic possibilities of the device

Fig. 2 shows the kinematic curves of the reaction

$$\pi^- + p \longrightarrow n + X^\circ$$

The curves corresponding to the different masses of X_o are shown in the above figure by elliptical arcs. The kinematic curves were plotted in the same way as in paper /4/. The momentum (the region between the arcs centred on point "O" and with radii of r_1 = 0,20 GeV/c and r_2 = 0,75 GeV/c) and angular (the radial lines drawn from point "O") captures of the X_o mass spectrum provided by the neutron detector are plotted in the above diagram. The solid curves and hatched curves correspond to the different masses of X^o at P_i = 40,0 GeV/c and P_i = 41,20 GeV/c (i.e. P_i + 0,03 P_i) respectively.

Thus, by plotting these curves, it is possible to determine the range of masses recorded by the neutron detector in various positions. In particular, with the detector in the position shown in Fig. 1: the range of θ angles = (60–80°) and the range of X^o masses defined by the neutron detector is (0–3) GeV/c^2.

We should point out that, with the introduction of a kinematic matrix into the neutron detector's electronic system, it is possible to define a specific region of momentum capture for each neutron counter within the general allowed momentum capture of the device, i.e. isolate sections where there are no mass curves in the (θ , pn) plane (for example, the hatched section in Fig. 2 between (80–82,5°).

Fig. 3 shows the geometrical efficiency in terms of θ with which different masses from the range (0–3) GeV/c are recorded when the detector is in the position shown in Figure 1.

The expected accuracy with which the time of flight of the neutron over L = 3 m is measured is $\sigma(\Delta\tau) = 0{,}5$ nsec; therefore, the device's momentum range may be divided into 30 regions:

(11.1) $\begin{cases} \text{from } p_n = 750 \text{ MeV/c} \longrightarrow \tau = 16 \text{ ns. to} \\ \quad\quad p_n = 200 \text{ MeV/c} \longrightarrow \tau = 48 \text{ ns ;} \end{cases}$

the angular accuracy with which the neutron's emission direction is determined (when an interaction point is re-established in the H_2 target) $\sigma(\Delta\theta) = \pm\, 0{,}6°$.

III Estimates of possible values for the effect and contribution of background reactions. Accuracies. Possibilities for data acquisition.

On the basis of (1.5), (1.6), (1.7), (1.8), and (1.11), the following conclusions may be drawn concerning the values of cross-sections at Pi = 40 GeV/c (table 1).

Table I

Pi(GeV/c)	$\sigma_{tot}(\pi^- p \to n\pi^+\pi^-) \sim p_i^{-1,3}$ (mb)	$\sigma(n\rho^0) \sim p_i^{-2}$ (microbarn)	$\sigma(nf^0) \sim p_i^{-2}$ (microbarn)	$\sigma(ng^0) \sim p_i^{-2}$ (microbarn)
II	0,7 ± 0,I0	II0 ± I4	75 ± I4	55 ± I4
I6	0,4 ± 0,08	52 ± I3	38 ± 9	25 ± 6
40	0,I ± 0,02	8 ± I,6	6 ± I,2	4 ± 0,8

Considering that

(III.2) $$\sigma_{tot}(\pi^- p \to n\pi^+\pi^-) \simeq 0,1 \text{ mb}$$

and assuming that (as in (1.10))

$$\frac{d\sigma}{dt} \sim e^{-10|t|}$$

we obtain

(III.2) $$\frac{d\sigma}{dt}\left[\mu б \cdot \left(\text{ГэВ}/c\right)^{-2}\right] \simeq e^{-10|t|}, \quad |t| \text{ в } \left(\text{ГэВ}/c\right)^2$$

and

(III.3) $$\sigma\Big|_{t_1}^{t_2} = 0,1\left(e^{-10|t_1|} - e^{-10|t_2|}\right) \mu б$$

that, if $\sqrt{|t_1|} = 0.2$ GeV/c, $\sqrt{|t_2|} = 0.64$ GeV/c

(p_{π^-} = 0,75 Бэв/ -cm (П-I) gives

$$\sigma\Big|_{t_1=-0{,}04}^{t_2=-0{,}40} \simeq 0{,}065\ \text{мб}$$

Considering that diagrams like

(III.4)

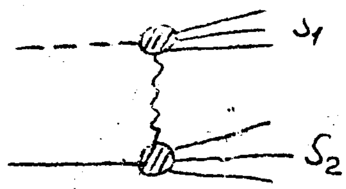

most likely at $S_1 \gtrsim 4\ (\mathrm{GeV}/c)^2$ do not contribute much to the cross-section /5/, it may be expected that

(III.5) $$\sigma\Big|_{-0{,}04}^{-0{,}40} \left(M_0 \leq 3\ \frac{\mathrm{GeV}}{c^2}\right) \simeq 0{,}06\ \mathrm{mb}$$
$$(\pi^- p \to n\pi^+\pi^-).$$

(We note that, as was shown in II, this range of /t/ momentum transfers and (M_0) missing masses is recorded by the device).

——— * ———

At a primary beam intensity of No = 10^5/cycle, a distance to the neutron spectrometer of L = 3m, a mean angle $\bar{\theta}$ n = 70°, with counters measuring 10 x 10 x 25 cm^3 (i.e. $d\Omega$ = 5.10^{-3}, mean efficiency $\bar{\varepsilon}$ = 3.10^{-1}), and using a hydrogen target of ℓ = 50 c.m. ($\ell\rho$ = 3.6 g/cm^2 of matter), the effect may be expected to be recorded as follows

(III.6) $$\mathcal{N}_1 = \mathcal{N}_0 \cdot \sigma \cdot \mathcal{E} \cdot d\vartheta \cdot l \cdot \rho \cdot \mathcal{N}_A =$$

$$= 10^5.6.10^{-29}.3,10^{-1}\ 5,10^{-3}.3,6.6.10^{23} = 2.10^{-2}/\text{cycle}$$

We note that clearly, with the neutron counters in the position given in II, all Υ-mesons from 2-, 3- and 4- particle decays of Mo will hit the magnetic spectrometer.

---------- * ----------

Before estimating the background, we shall indicate the accuracy of the apparatus and how this contributes to the accuracy with which Mo and /t/ are measured.

The accuracy with which the neutron's time of flight is measured is

(III.7) $$\sigma(\Delta\tau) \sim 0,5 \text{ ns}$$

The accuracy with which the neutron's coordinates (in terms of θ) are determined when an interaction point is re-established in the target is

(III.7[1]) $$\sigma_\theta \sim 3\text{cm}$$

It may be shown that there is little contribution from the dimensions of the targetand counter to the accuracy with which p_n (or β_n) is measured at a momentum of 200 MeV/c $\leq p_n \leq$ 750 MeV/c and at $\bar{\theta}_n \sim 70^\circ$.

We shall assess the contribution to ΔM_0 of the accurate measurements of $\Delta\tau$ and $\Delta\theta$ at $\sigma\left(\frac{\Delta p_i}{p_i}\right) \sim 0,5\%$ and at mean values of M_0, p_n and θ_n (hence $p_i \equiv p_1$).

The neutron's missing mass in the reaction $\pi^- + p \rightarrow n + M_0$

(III.8)
$$\pi^- + p \rightarrow n + M_0$$
$$M_0^2 = 2m_n^2 + 2p_n p_1 \cos\Theta_n - 2p_1(m_n + E_n) - 2E_n m_n + \mu_\pi^2$$

where p_n, m_n, E_n and Θ_n are the momentum, mass, energy and emission angle of the neutron relative to the direction of the primary beam and p_1 is the momentum of the incident meson in the laboratory system, ($m_n \simeq m_p$).

From (III.8) it is easy to obtain

(III.9)
$$\frac{dM_0}{M_0} = k_1\, d\beta_n/\beta_n + k_2 \frac{dp_1}{p_1} + k_3\, d\Theta_n$$

where

(III.9)
$$\begin{cases} k_1 = \dfrac{m_n}{M_0^2} \dfrac{\beta_n}{(1-\beta_n^2)^{3/2}} \left[p_1 \cos\Theta_n - (p_1 + m_n)\beta_n\right] \\[2ex] k_2 = \dfrac{m_n + p_n \cos\Theta_n - E_n}{M_0^2}\, p_1 \\[2ex] k_3 = \dfrac{p_n p_1}{M_0^2} \sin\Theta_n \end{cases}$$

We put into (III.9) and (III.9[1]) p_1 = 40 GeV/c, $\Theta_n = 70^\circ$ and M_0 = 2,0 GeV/c^2;

then

p_n = 0,470 GeV/c, β_n = 0,454, E_n = 1,036 GeV and

(III.10) $dM_0/M_0 \sim$ 10,5% at the above accuracies of (III.7) and (III.7[1]) i.e.

(III.10) $dM_0 \sim$ 210 MeV/c^2

We note that the mean accuracy for measuring $p_n \simeq \sqrt{-k}$ in our range from 200 to 750 MeV/c

(III.11) $$\frac{dp_n}{p_n} = \frac{d\beta_n}{\beta_n}\frac{1}{(1-\beta_n^2)^{3/2}} \sim 2.10^{-2}, \text{ i.e.}$$

(III.11[1]) $$dp_n \simeq 10 \text{ MeV/c, and}$$

(III.11[11]) $$dt \sim 0{,}01\ (\text{GeV/c})^2$$

Background reactions

The main background reaction for (1.1), following on from the diagram with a charged pole exchange, is the reaction

(III.13)
$$\pi^- + p \to N^* + \pi^-$$
$$\quad\quad\quad\quad\quad \llcorner\!\to n\pi^+$$

which is described by the following diagram

(III.14)

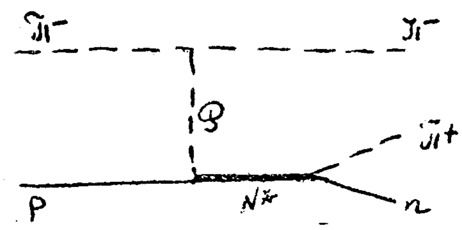

with a vacuum pole exchange. The cross-section of this process is of the order of tens of millibarns /6/, /7/, yet its contribution must be small as the π^+ from the decay of N^* are soft.

The contribution from the reaction

(III.15)
$$\pi^- + p \to n + \pi^+ + \pi^- + \pi^0$$

An analysis of the momentum balance at

* $$\frac{dp_1}{p_1} \simeq 0{,}5\%\,, \quad \frac{dp_n}{p_n} \simeq 2\%\,, \quad \frac{dp_+}{p_+} = \frac{dp_-}{p_-} \simeq 1\%$$

shows that there is a background contribution of reaction (III.15) at $p_{\pi^0} \lesssim 500$ MeV/c.

If reaction (III.15) follows the diagram

(III.15[1])

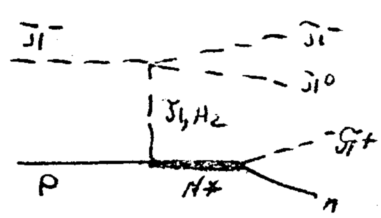

with a cross-section $\sim$ one order greater than that investigated, the background contribution (p_{π^0} = 0,5 GeV/c) may be expected to be (1-2)%. If reaction (III.15) follows the diagrams for charged-pole exchange

(III.15)

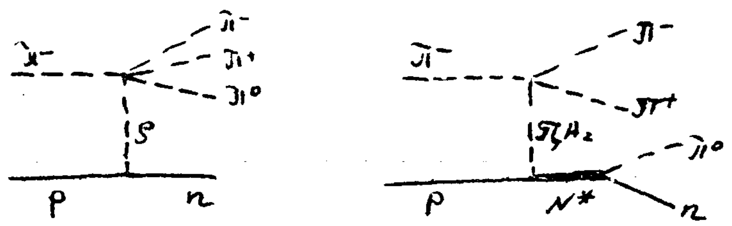

then $$\sigma(\pi^- p \to n\pi^+\pi^-)$$

1) its cross-section is a decreasing function of energy and should have the same order of magnitude as

2) 1% background contribution may be expected from the left-hand diagram when there is an isotropic distribution of π -mesons in the c.m.s. of the 3π system.

3) background from the right-hand diagram may be suppressed by a factor of $\sim$ 3.5 using γ -quanta anticoincidence counters on three sides of the target. Moreover, the accuracy with which the missing mass of the $\pi^+\pi^-$ system is re-established should be sufficient to suppress the background from this process.

We note that the reactions

$$\pi^- + p \to n\pi^+\pi^-$$

and

$$\pi^- + p \to np\bar{p}$$

are well defined when the momentum and mass balances are calculated with the accuracy shown in (*).

In order to make a clearer division between the reactions

$$\pi^- + p \to n\pi^+\pi^-$$

and

$$\pi^- + p \to nK^+K^-$$

it is essential to increase the accuracy of the $\frac{dp^{\pm}}{p^{\pm}}$ measurements to $\sim$ (0.3 to 0.5)%; this is within the capabilities of the MAGIK-6.

Data acquisition rate.

Trigger efficiency.

As can be seen from (III.6), at $N_0 = 10^5$/cycle, the $(n\pi^+\pi^-)$ effect will be recorded at the rate of 1/50 cycles. However, using the electronic logic shown in fig.1, triggering will also give the reactions

$$\text{(III.16)} \quad \begin{cases} \pi^- + p \rightarrow n + m(\pi^+\pi^-) + k\pi^0 \\ \pi^- + p \rightarrow n + m(K^+K^-) + k\pi^0 \\ \pi^- + p \rightarrow n + m(p\bar{p}) + k\pi^0 \end{cases} \qquad \begin{matrix} m \geq 0,\ k > 0 \\ m > 0,\ k \geq 0 \end{matrix}$$

Therefore, the number of triggers may be expected to be 1/1 to 1/5 cycles (assuming that the cross-sections of the (III.16) reactions are of the order of tens of microbarn.).

In this case, π°-mesons from the reactions

$$\text{(III.17)} \quad \pi^- + p \rightarrow \begin{cases} n + \pi^+\pi^-\pi^0 \\ n + \pi^+\pi^-\pi^+\pi^- \end{cases}$$

also hit the MAGIK-6 and these processes may be analysed.

In order to obtain $\sim 10^3$ $n\pi^+\pi^-$ events (573 events in paper /3/ at $p_{\pi} = 16$ GeV/c) $\sim$ 100 hours of machine time are required.

The number of photographs may be estimated at 10-50 thousand, of which about 5 thousand showing two charged particles are being measured.

Further development of the device.

1. If the total number of triggers is going to be 1/5 cycles, then the luminosity of the neutron detector should be increased.

This may be done in one of the following ways:

1) increase the size of each detector to 12 x 50 x 25 cm^3,

2) increase the number of channels to 16.

Alternative 1) requires no additional electronic equipment, whilst alternative 2) calls for ~ 20% more. To increase the size of the counters, it is essential to have time photomultipliers with large photocathodes of the RTXP 1041 (1040, 58 AVP) type, block scintillation plastic 13 x 52 x 26 cm^3 and also block optical plastic (light guides) 13 x 51 x 51 cm^3.

II. The data-processing rate may be increased by adding a Facit-4070 tape punch (made in Sweden). The data can also be fed on-line to a digital computer.

All the members of the MAGIK-6 group will also take part in the various stages of this experiment.

Bibliography

1. B. French. 14th International conference on high-energy physics. Vienna 1968 p. 91.

2. C. Caso et al. Nuovo cim. 42a N 3 (1969).

3. J. Billam et al. Ph. Lett. 31B №7 64897 (1970).

4. I. Blaton. Geometricheskaya interpretatsiya sokhraneniya energii i impul'sa v atomnykh stolknoveniyakh i protsessakh rasshchepleniya.

   (A geometrical interpretation of the conservation of energy and momentum in atomic collisions and fission processes.)

5. A.B. Kajdalov. Obrazovanie chastits pri vysokikh energiyakh i vetvleniya v uprugom NN, N and KN rasseyanii.

   (Particle production at high energies and branching in elastic NN, N and KN scattering.)

   To be published in Yadernaya Fizika.

6. K.J. Foley et al. Ph. Rev. Lett. 19 (1967) 397.

7. W.D. Walker et al. Ph. Rev. Lett. 20 (1968) 133.

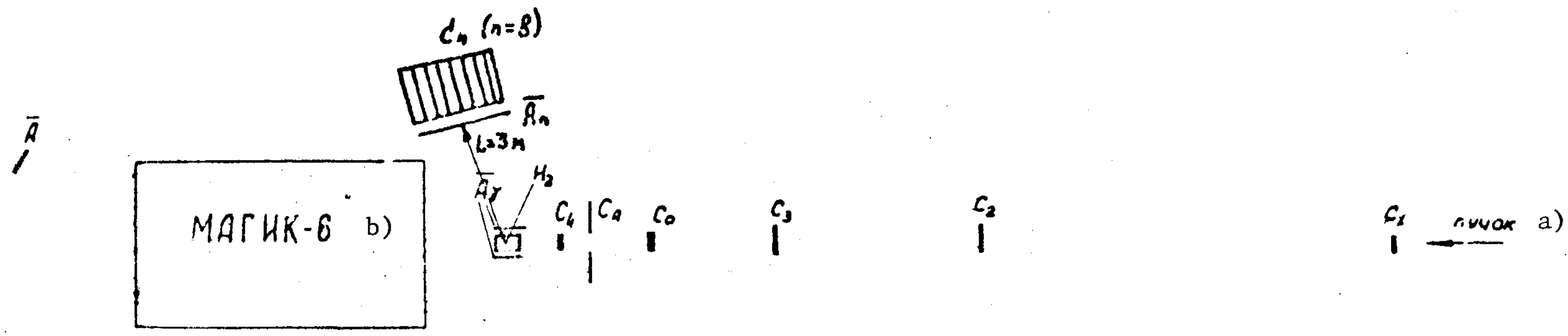

$$T = \left[C_1 C_2 C_3 C_4 \overline{C_A}\right] \times C_0 \times \sum_{\ell=1}^{4} \overline{A_\gamma}^{\ell} \left\{\left[\sum_{k=1}^{8} C_n^k\right] \times \overline{\left[C_n^s \cdot C_n^t\right]}_{s \neq t} \times \left[\sum_i \overline{A_n^i}\right]\right\}$$

Fig. 1. Position of the apparatus in the particle beam, trigger's electronic logic.

a)- beam
b)- MAGIK-6.

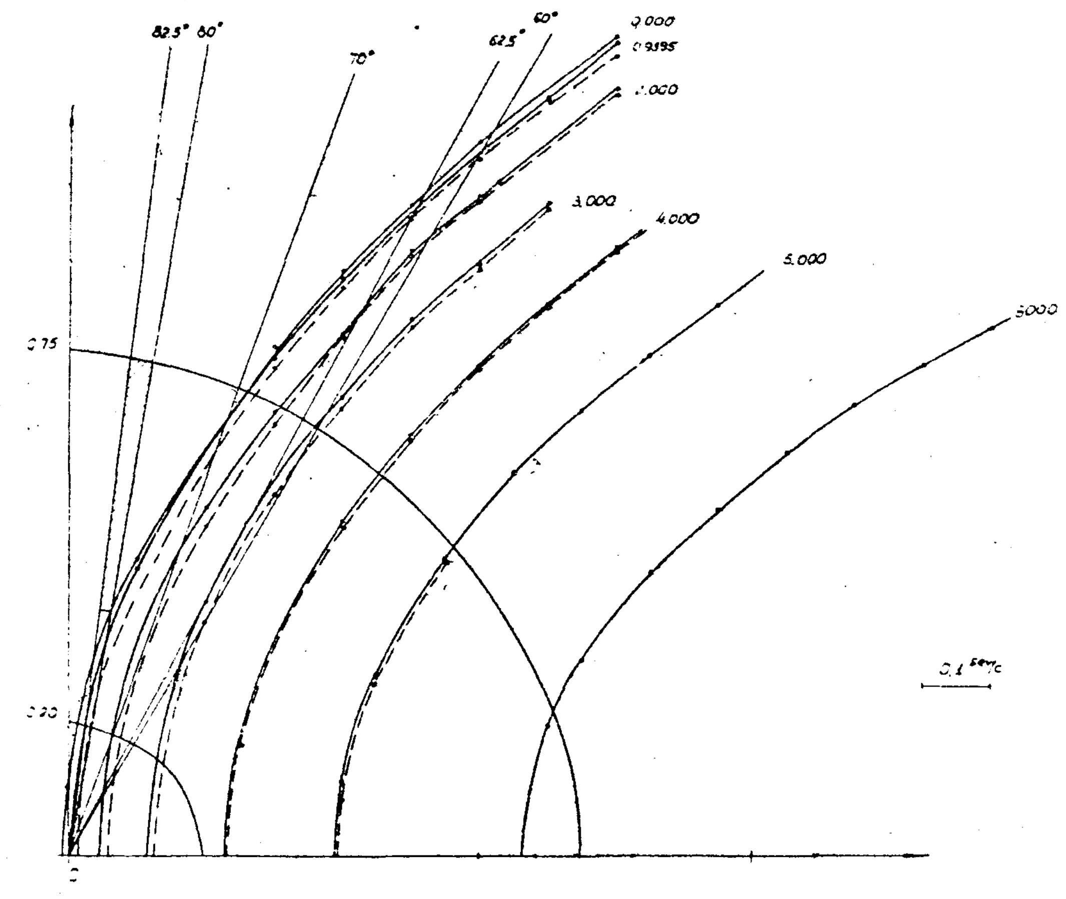

Fig. 2. Kinematic curves of the reaction $\pi^- + p \rightarrow n + \mu_0$

Solid ellipses p_i = 40 GeV/c
Hatched ellipses p_i = 41,2 GeV/c

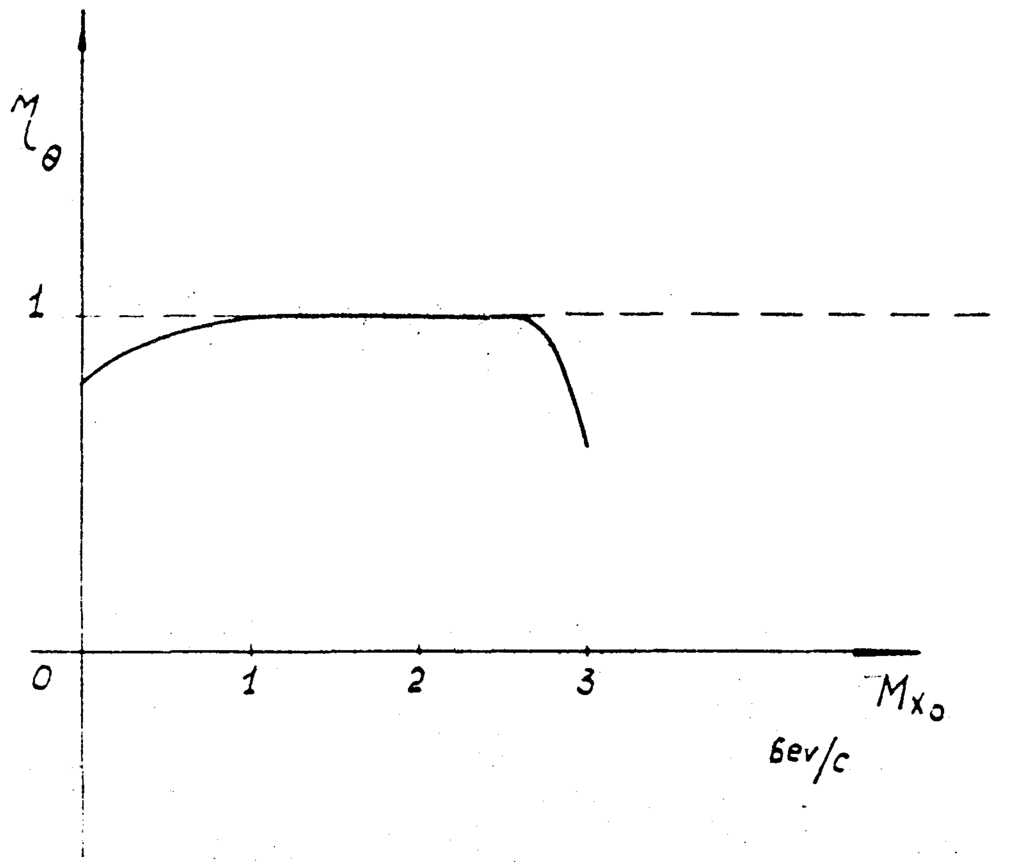

Fig. 3. Geometrical efficiency in terms of the angle of the neutron spectrometer against the missing mass M_x.